PHYSICAL REVIEW B VOLUME 47, NUMBER 16 15 APRIL 1993-II

Screening and exchange in the theory of the femtosecond kinetics of the electron-hole plasma

J. H. Collet
Departement de Physique, Institut National des Sciences Appliquées, Université Paul Sabatier, avenue de Rangueil 31077 Toulouse, France
(Received 19 May 1992; revised manuscript received 23 November 1992)

This work deals with the dynamics of the nonthermalized electron-hole plasma in the subpicosecond regime. We computed different collision rates (electron-electron, electron-hole, electron-phonon) and discussed the relative efficiency of the different processes for the cases of static or dynamic screening of the interaction. We also considered how the inclusion of the exchange affected the scattering amplitude and the collision rates. Calculations were based upon GaAs. We conclude that dynamic screening is crucial for electrons in the conduction band at a high plasma density [say, at densities above $(1-2)\times 10^{16}/\mathrm{cm}^3$], whereas it generally plays a minor role at low density and when descibing hole dynamics. The excitation of heavy holes into the light-hole band by collisions with the conduction electrons is discussed in heavily p-doped GaAs.

I. INTRODUCTION

The relaxation of nonequilibrium electron-hole plasmas (EHP's) in the subpicosecond regime has been investigated for about 10 years in direct-gap semiconductors. Experimental methods using an optical excitation have played a crucial part in these investigations since subpicosecond pulses enable the direct generation of nonthermalized EHP's. The first studies concerned the modulation of the transmission close to the band edge. These investigations have been continuously extended to many direct-gap semiconductors [for instance, GaAs,[1,6] InP,[7] GaAlAs (Refs. 8–10)]. Time-resolved Raman spectroscopy has also been investigated [GaAs (Ref. 11)]. Time-resolved luminescence techniques appeared more recently and are continuously being refined.[12–18] An understanding of the optical properties of a strongly excited EHP in terms of microscopic plasma theory may be tentatively described as a three-step process involving the following steps.

(1) Observation of some optical property of the excited EHP (time-resolved absorption, luminescence, etc.).

(2) Analysis of the experimental data. This step mostly concerns the extraction of information on the distribution functions, the electron-hole correlations, the screening, etc., from the analysis of the absorption (or the luminescence) line shape.

(3) Development of a plasma dynamics theory (if possible without any adjustable parameter) to account for the subpicosecond kinetics of the critical parameters deduced during the two previous stages.

Our separation of steps 2 and 3 is somewhat arbitrary. Step 2 is not simple. The interpretation, for example, of transmission experiments close to the band edge must take into account the electron-hole correlations, the exciton screening, and the particle damping. An introduction to the optical properties of the EHP (in thermal equilibrium) may be found in Refs. 19 and 20. Step 3 is a standard problem of nonequilibrium statistical mechanics (NESM) that has been extensively studied since the pioneering work of Boltzmann in 1872.[21] Many physicists have contributed to the development of NESM, especially the derivation of the Boltzmann equations, and the discussion of their range of application. An extended review of the subject can be found in Ref. 22. Field-theoretical methods have also been used.[23–25]

Three main theoretical approaches prevail in the literature describing the EHP dynamics in semiconductors. In a first approach, investigations start from the very general equations of the nonequilibrium quantum statistical mechanics (Balescu-Resibois formalism,[26] time-dependent Green's functions[23–25,27–30]). This ambitious approach may in principle describe both the coherent and incoherent interaction of electrons with subpicosecond optical pulses. But so far, it has (apparently) not succeeded in really calculating the subpicosecond kinetics of observable quantities because the solution of the Green's-function equations of motion lead to extremely arduous numerical computations when correlations and screening are included. The fundamental problem consists of finding a compromise between the formal aspects of the theory and the real computation capabilities. Nevertheless, these works are interesting because they suggest an exact treatment. In a second approach, the investigations start from Boltzmann-like kinetic equations and develop complex but still tractable numerical computations. These works are directly related to the first approach because the Master and Boltzmann's equations can be derived from the theory of nonequilibrium Green's functions within the framework of the so-called quasiparticle approximation. The numerical results have been compared to experimental data.[31–33] Now this second approach is limited to the semiclassical regime, i.e., when the plasma dynamics are controlled by collision effects rather than by coherent quantum effects. Fortunately, it turns out that this condition is often satisfied in the subpicosecond regime, when the plasma density is typically larger than $10^{17}/\mathrm{cm}^3$. In a third approach, the carrier dynamics have been described by Langevin equations and then solved by the Monte Carlo method. These methods

are in principle equivalent to directly solving the Boltzmann equations (second approach). However, they require very long computation times to attain some accuracy.[34–38]

This work is essentially devoted to discussing plasma dynamics in GaAs when the initial kinetic energy of the electron is of the order of 100–200 meV. The EHP is mostly confined in the Γ valley. Our first calculations of plasma dynamics[31,32] (within the framework of a two-band model and static screening) predicted the observation of a clear hole-burning effect in GaAs in subpicosecond regime at plasma density around $(6-7)\times 10^{17}/\mathrm{cm}^3$ when generating the EHP with 500-fs pulses. Several experimental results show that the observation of this effect is not so pronounced (see for instance Ref. 5). This means that our initial treatment underestimated the efficiency of carrier-carrier scattering. We therefore wish to develop a more sophisticated model that includes a dynamic screening of the Coulomb interaction and the two valence bands.

The manuscript is organized as follows: We recall plasma kinetic equations in Sec. II and emphasize the way in which we screen the interactions. We show that information on the sensitivity of scattering processes to dynamical effects may be deduced from the calculation of the dielectric function and from the inspection of the material band structure. We derive in Secs. III and IV the expressions for the different carrier-carrier scattering rates. Several scattering rates are computed in Sec. V for conduction electrons both for static and dynamic screening. We show the impact of the approximations. Computations are conducted for GaAs which has been by far, the most studied direct-gap material to date. The following conclusions stress the importance of the dynamic screening.

a. Intrinsic GaAs, photogeneration energy 60–70 meV above the band edge.

(i) Electron-electron scattering. The inclusion of a dynamic screening is essential for the computation of this collision rate at densities above $(1-2)\times 10^{16}/\mathrm{cm}^3$. At low density, typically below $5\times 10^{15}/\mathrm{cm}^3$, the dynamic and the static screening approximations give similar results. The consideration of the exchange term in the matrix element of the electron-electron interaction gives rise to a weak enhancement of the scattering rate.

(ii) Scattering by emission-absorption of bare LO phonons or mixed modes. The two theories lead to similar results. The relative scattering rate at the photogeneration energy is quasiconstant around 5 ps^{-1} for plasma densities ranging from 10^{15} to $10^{18}/\mathrm{cm}^3$. The simple theory of *bare* LO-phonon emission without screening is reasonably good up to $(3-4)\times 10^{17}/\mathrm{cm}^3$.

(iii) The static screening generally holds for H-H processes (heavy-hole–heavy-hole collisions).

b. n-doped GaAs (hole density small compared to that of electrons, i.e., $\rho_h \ll \rho_c$). A description of the plasma dynamics reduces to a study of the thermalization and the cooling of holes. Conduction electrons remain quasithermalized at the bath temperature. The static screening approximation generally holds when describing hole-hole collisions and LO-phonon emission.

c. Weakly excited p-doped GaAs (electron density small compared to that of holes, i.e. $\rho_e \ll \rho_h$). In this case, the description of the plasma dynamics reduces to studying the internal thermalization and the cooling of the conduction electrons. Holes remain quasithermalized at the bath temperature. The dynamic screening model of the electron-electron and electron-LO processes is necessary. In heavily *p*-doped material ($\rho_h > 10^{19}/\mathrm{cm}^3$), the relaxation of the conduction electrons by direct excitation of heavy holes into the light-hole band becomes the dominant intraband relaxation process (*C*-HL process).

II. KINETIC EQUATIONS AND SCREENING

We use Boltzmann equations to describe the kinetics of one-particle distribution functions. A distribution function is associated with each carrier band and with each optical phonon type. The temporal evolution of the distributions is described by a system of coupled integro-differential equations. If, for example, we consider one conduction band, two valence bands, and LO phonons, then we may describe the system using the following set of equations:

$$\frac{df_c}{dt}=g_C+\left.\frac{df_c}{dt}\right|_C+\left.\frac{df_c}{dt}\right|_H+\left.\frac{df_c}{dt}\right|_L+\left.\frac{df_c}{dt}\right|_{\mathrm{LO}}, \tag{1a}$$

$$\frac{df_H}{dt}=g_H+\left.\frac{df_H}{dt}\right|_H+\left.\frac{df_H}{dt}\right|_L+\left.\frac{df_H}{dt}\right|_C+\left.\frac{df_H}{dt}\right|_{\mathrm{LO}}, \tag{1b}$$

$$\frac{df_L}{dt}=g_L+\left.\frac{df_L}{dt}\right|_L+\left.\frac{df_L}{dt}\right|_H+\left.\frac{df_L}{dt}\right|_C+\left.\frac{df_L}{dt}\right|_{\mathrm{LO}}, \tag{1c}$$

$$\frac{db_{\mathrm{LO}}}{dt}=\left.\frac{db_{\mathrm{LO}}}{dt}\right|_H+\left.\frac{db_{\mathrm{LO}}}{dt}\right|_L+\left.\frac{db_{\mathrm{LO}}}{dt}\right|_C, \tag{1d}$$

where f_C, f_H, f_L, b_{LO} are the one-particle distribution functions, respectively, for the conduction electrons, the heavy holes, the light holes, and the LO phonons. g_C, g_H, and g_L are the generation rates under optical excitation in the conduction band, and in the heavy- and light-hole bands, respectively. The other terms of the right-hand side represent the scattering rates due to the different scattering processes. For instance $(df_C/dt)|_H$ is the scattering rate in the conduction band due to the collisions of electrons with heavy holes (*C*,*H* subscripts). The first crucial point that must be clarified is the range of application of these equations. It is well known from the dynamic derivation of the Boltzmann equation[22,25,39] that one-particle distributions are related to many-particle distributions within an infinite hierarchy of equations. Now, many-particle functions become functionals of the single one-particle distributions, i.e., the system loses memory, for time $\Delta t > t_0$, where t_0 is the duration of a single collision. Boltzmann's equations hold in this limit. The duration t_0 of a collision may be estimated as[25,39]

$$t_0 \approx 1/q_D \bar{v}_{\rm th} \tag{2}$$

with

$$q_D^2 = \frac{4\pi e^2}{\varepsilon_\infty q^2} \sum_{\sigma,k,i} \frac{\partial f_i(E)}{\partial E} ,$$

where q_D is the Debye-Hückel wave vector and $\bar{v}_{\rm th}$ the average velocity of carriers. It turns out that the condition $\Delta t > t_0$ is satisfied after a few tens of femotoseconds when the plasma density is larger than $10^{17}/{\rm cm}^3$ (see Appendix A). As a result, Boltzmann's equations often are expected to provide a reasonable description of the kinetics of the one-particle distributions in the subpicosecond regime. The different scattering terms of the right-hand side of Eqs. (1) may be case in a common form which reads

$$\left. \frac{d}{dt} f_i(k) \right|_j = -f_i(\mathbf{k}) S_{i,j}^-(k) + [1 - f_i(\mathbf{k})] S_{i,j}^+(k) . \tag{3}$$

This decomposition simply describes the competition between the processes that scatter carriers out of the k state (first term) and those that scatter carriers into the k state (last term). The explicit form of factors $S_{i,j}^{\pm}$ depends on the scattering process between the bands i and j. Let us consider for example the emission of *bare* LO phonons. We get for $S_{i,j}^+$

$$S_{i,j}^+(k) = \frac{2\pi}{\hbar} \sum_{q,\nu=\pm} f_j(\mathbf{k}-\mathbf{q}) \left| M_{ij} \right|^2 \left[\frac{1}{2} - \nu \frac{1}{2} + b_{\rm LO}(q) \right] \times \delta[\Delta E_{ij}(q,k) - \nu \hbar \omega_{\rm LO}] , \tag{4}$$

where $\mathbf{q}$ and $\Delta E_{ij}(q,k) = E_i(\mathbf{k}) - E_j(\mathbf{k}-\mathbf{q})$ are, respectively, the wave vector and the energy exchanged in the scattering process. One crucial aspect of kinetic equations concerns the structure of the scattering amplitude M_{ij}. Simple intuitive considerations suggest the use of the matrix element of bare binary interactions. For the emission of bare LO phonons that we have just considered, the matrix element depends both on the input and output wave vectors of the carrier ($\mathbf{K}$ and $\mathbf{K}+\mathbf{q}$) and reads

$$|M_{ij}(\mathbf{K},\mathbf{K}+\mathbf{q},\Delta E)|^2 = |V_{\rm LO}(q)|^2 C_{ij}(\mathbf{K},\mathbf{K}+\mathbf{q}) , \tag{5}$$

where $|V_{\rm LO}(q)|^2 = (4\pi e^2/q^2)(1/\varepsilon_0 - 1/\varepsilon_\infty)/(\hbar\omega_{\rm LO}/2)$ is the standard matrix element of the Fröhlich interaction. The coefficients $C_{ij}(\mathbf{K},\mathbf{K}+\mathbf{q})$ are due to the overlap of the cell periodic part of the initial and final Bloch functions involved in the scattering process. The main coefficients are $C_{\rm CC}$ for the conduction-conduction transitions, $C_{\rm HH}$ and $C_{\rm LL}$ for intravalence band scattering in the heavy- or light-hole band, respectively, $C_{\rm LH}$ and $C_{\rm HL}$ for intervalence band scattering. The overlap factors close to the Γ point have been derived in Ref. 40. They read

$$\begin{aligned} C_{\rm CC} &= 1 , \\ C_{\rm HH} &= C_{\rm LL} = (1 + 3\cos^2\chi)/4 , \\ C_{\rm LH} &= C_{\rm HL} = 3\sin^2(\chi)/4 , \end{aligned} \tag{6}$$

where χ is the angle between the vectors $\mathbf{k}$ and $\mathbf{k}+\mathbf{q}$.

Now bare interactions may lead to divergent integrals $S_{ij}^{\pm}$ (for instance, for the Coulomb potential). This is clear evidence that they are not satisfactory. As was extensively discussed in several textbooks,[25,26,39] M_{ij} is in fact related to the vertex function of the scattering process. A possible approximation of the vertex consists of screening the bare interaction $V_{ij}(q)$ by using the longitudinal dielectric function of the plasma.[25,39] We get

$$|M_{ij}|^2 \approx \frac{|V_{ij}(q)|^2}{|\varepsilon[q,\Delta E_{ij}(q)]|^2} , \tag{7}$$

where $\Delta E_{ij}(q)$ is again the energy which is exchanged in the collision. For electron-hole plasmas, the longitudinal dielectric constant is best described in the random-phase approximation (RPA) which reads.[42,43]

$$\varepsilon(q,\hbar\omega) = 1 - \frac{4\pi^2}{\varepsilon_\infty q^2} \sum_{K,\alpha,\beta} C_{\alpha\beta}(\mathbf{K},\mathbf{K}+\mathbf{q}) \frac{f_\alpha(\mathbf{K}+\mathbf{q}) - f_\beta(\mathbf{K})}{\hbar\omega - E_\alpha(\mathbf{K}+\mathbf{q}) - E_\beta(\mathbf{K}) - i\eta} . \tag{8}$$

The subscripts α,β run over all the excited bands. In the static limit $\hbar\omega = 0$ and for small q, the RPA dielectric function of the plasma reduces to following the simple expression:

$$\varepsilon(q,0) = 1 + \frac{q_D^2}{q^2} , \tag{9}$$

where q_D is again the Debye-Hückel wave vector [Eq. (2)]. Now, it must be clearly stressed that the utilization of this *static* limit in the scattering amplitude [Eq. (7)] only holds if the exchanged energy $\Delta E_{ij}(q)$ is small compared to that of the plasmon. Many works on the Mott transition of excitons and on electron-hole liquids in semiconductors have demonstrated that the static approximation strongly overestimates screening (for a review, see for instance Ref. 19). In other words, the static screening approximation underestimates the carrier-carrier interactions. If the static approximation has been systematically used in plasma kinetics problems,[31–36] this is for technical reasons, i.e., because the expression of the dielectric function reduces to the simple form of Eq. (9) that is compatible with the heavy computations involved in the numerical treatment. The obvious difficulty, concerning the dynamic screening approximation, is that the real part of the RPA dielectric function [from Eq. (8)] is a difficult integral. It can always be computed for a specific study on screening (see, for instance, Ref. 43), but it is too time consuming when it is involved in a more general program of plasma kinetics. A possible compromise for including dynamic screening in kinetic equations consists of using the plasmon pole approximation (PPA) which is

a simplified analytic version of the RPA. It has been previously used for studying plasmas and electron-hole liquids in semiconductors.[19,44,45] The expression of the dielectric function in this approximation is

$$\varepsilon(q,\hbar\omega)=1-\Pi_c(q,\hbar\omega)-\Pi_h(q,\hbar\omega)\ , \tag{10}$$

where Π_e and Π_h are the approximated polarization kernels of the conduction and valence bands which read

$$\Pi_i(q,\hbar\omega)=\frac{\omega_{\mathrm{pl},i}^2(0)}{\omega^2-\omega_{\mathrm{pl},i}^2(q)+\omega_{\mathrm{pl},i}^2(0)-\Delta_i^2(q)-2i\omega\Delta_i}\ . \tag{11}$$

$\omega_{\mathrm{pl},i}(0)$ is the plasmon energy at $q=0$ in the band i. We recall that $\omega_{\mathrm{pl},i}^2(0)=4\pi e^2\rho_i/\varepsilon_0 m_i$ where ρ_i and m_i are the density of carriers and the carrier mass in the band i, respectively. The damping coefficient Δ_i is approximated by the expression $\Delta_i=\Gamma\omega_{\mathrm{pl},i}$ where Γ is of the order of 0.2–0.3.[45] The following approximated dispersion curve of plasmon is used in the PPA:

$$\omega_{\mathrm{pl},i}^2(q)=\omega_{\mathrm{pl},i}^2(0)\left[1+\frac{q^2}{{q_{D,i}}^2}\right]\ . \tag{12}$$

$q_{D,i}$ is the Debye-Hückel wave vector for the band i. The details of the valence bands are not included when computing the polarizability [Eq. (11)], i.e., the valence bands are described by a single parabolic band. In the limit $\hbar\omega=0$, the PPA [Eqs. (10)–(12)] reduces to the static screening [Eq. (9)]. We plotted, in Figs. 1 and 2, the variations of the screening factor $1/|\varepsilon(q,\Delta E)|^2$ [see Eq. (7)] for GaAs at $T=300$ K in the presence of an EHP of density $\rho=10^{17}/\mathrm{cm}^3$. The RPA and the PPA are displayed in Figs. 1 and 2, respectively. The plasmon energy $\hbar\omega_{\mathrm{pl}}(0)$ equals 14 meV at $\rho=10^{17}/\mathrm{cm}^3$. The PPA obviously does not perfectly reproduce the RPA but the crucial features of the RPA dielectric function are well accounted for, as follows.

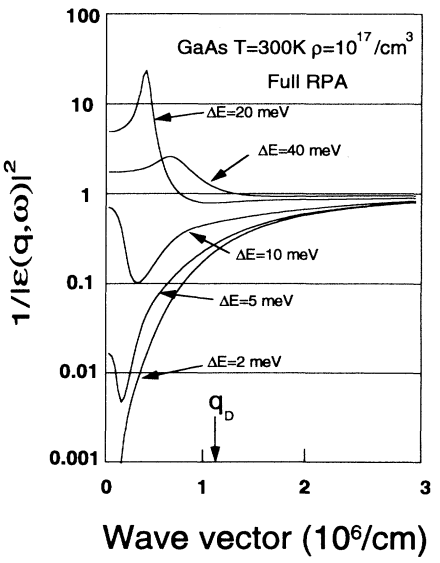

FIG. 1. Computation of $1/|\varepsilon(q,\Delta E)|^2$ in the RPA for GaAs at 300 K. $\rho_e=\rho_h=10^{17}/\mathrm{cm}^3$. The plasmon energy is $\hbar\omega_{\mathrm{pl}}$ 14 meV.

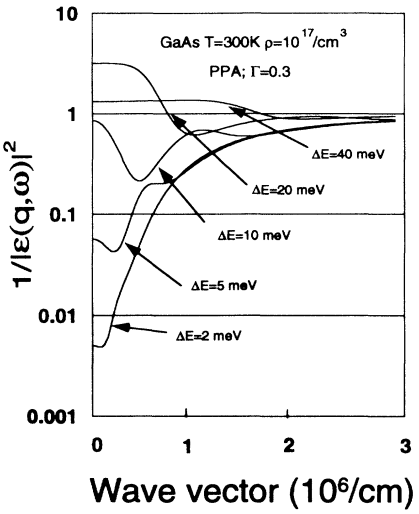

FIG. 2. Computation of $1/|\varepsilon(q,\Delta E)|^2$ in the RPA for GaAs at 300 K. $\rho_e=\rho_h=10^{17}/\mathrm{cm}^3$. The damping Δ_i [see Eq. (11)] is determined using $\Delta_i=\Gamma\omega_{\mathrm{pl},i}$ with $\Gamma=0.3$.[40] The plasmon energy is $\hbar\omega_{\mathrm{pl}}$ 14 meV.

(1) If $q\gg q_D$ then $\varepsilon\approx 1$ (see Fig. 1). The consequence for plasma dynamics is the following: If a scattering process mostly involves the exchange of a wave vector larger than the Debye-Hückel vector, the static and dynamic screening approximation will give similar results. In that case the screening model is not essential. This conclusion generally holds at low plasma density (say, typically when the density is below $10^{16}/\mathrm{cm}^3$ in GaAs) because the screening wave vector converges to zero.

(2) If $q\leq q_D$, then (a) if $\Delta E\gg\hbar\omega_{\mathrm{pl}}$, then $\varepsilon\approx 1$. Again dynamic and static screening provide similar results. (b) If $\Delta E\approx\hbar\omega_{\mathrm{pl}}$, then $\mathrm{Re}(\varepsilon)\approx 0$ so that $1/|\varepsilon|^2\gg 1$. The consequence for plasma dynamics is the following: If a scattering process mostly involves the exchange of a wave vector smaller or of the order of the Debye-Hückel vector and also the exchange an energy close to that of the plasmon, dynamic effects are expected to greatly enhance the magnitude of the scattering rate. Then it becomes crucial to use a dynamic screening. (c) $\Delta E\ll\hbar\omega_{\mathrm{pl}}$, the dielectric function reduces to the static expression. This condition is fulfilled for instance by the lines corresponding to $\Delta E=2$ meV (whereas $\hbar\omega_{\mathrm{pl}}=14$ meV) in Figs. 1 and 2. They are therefore almost identical with that obtained from the exact static screening.

The PPA certainly provides an improved description of the dielectric function with respect to the static approximation. The different curves in Fig. 1 display the enhancement of the transition probability in dynamic screening (with respect to the static screening) when the exchanged wave vector and energy are respectively of the order of the Debye-Hückel wave vector (here $q_D\approx 10^6/\mathrm{cm}$) and 20–40 meV. A quick look at the band structure of GaAs (Fig. 3) shows that these conditions are fulfilled for the relaxation of electrons high in the con-

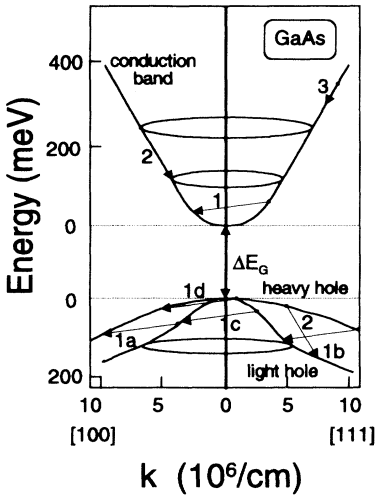

FIG. 3. Band structure of GaAs.

duction band (process 3). The particular energy $\Delta E = 36$ meV is that of the LO phonon. We therefore conclude from this study of the RPA dielectric function that the emission of LO phonons by electrons high in the conduction band is expected to be sensitive to dynamic effects. We discuss now a second example of transitions sensitive to dynamic screening effects. We plotted in Fig. 4 the variation of $1/|\varepsilon(q,\Delta E)|^2$ in different p-doped GaAs when the energy exchanged in the collision is $\Delta E = 70$ meV. This energy is roughly that of the splitoff between the heavy- and light-hole bands for a large wave vector in the direction [1,0,0] (see Fig. 3). The factor $1/|\varepsilon|^2$ was computed for several hole densities ranging from $10^{17}/\text{cm}^3$ to $8\times10^{18}/\text{cm}^3$. When the density is lower than $10^{18}/\text{cm}^3$, $\varepsilon \approx 1$ because $\Delta E \gg \hbar\omega_{\text{pl}}$. The resonance

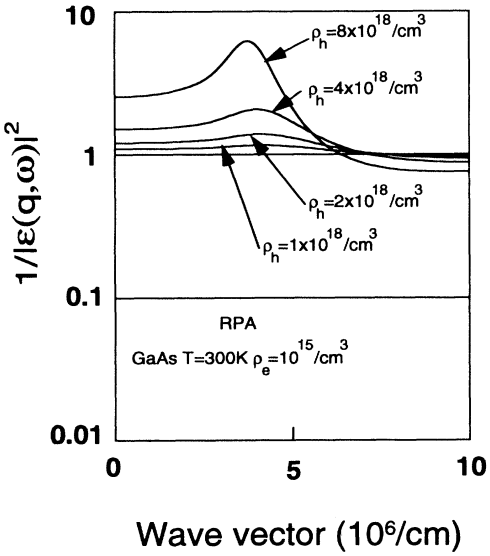

FIG. 4. Computation of $1/|\varepsilon|^2$ in the RPA for p-doped GaAs at 300 K for different hole densities. The electron density is constant at $\rho_e = 10^{15}/\text{cm}^3$.

of the splitoff energy ΔE with that of the valence plasmon occurs around the density $\rho \approx 2.5\times10^{19}$ cm^3 and leads to a large enhancement of the transition probability when the vector which is exchanged in the collision is of the order of (or smaller than) the Debye-Hückel wave vector $q_D \approx 5\times10^6/\text{cm}$. Again a quick look at the valence band in Fig. 3 shows that the electron-hole collisions accompanied by an intervalence band scattering of the hole such as for the process 2 fulfill these conditions. This electron-hole process is therefore expected to be sensitive to dynamic effects in heavily p-doped samples. These two examples demonstrate that an initial conclusion about the sensitivity of the scattering processes to dynamic effects can be reached from the calculation of the dielectric function and from the inspection of the band structure. Now the final conclusion comes from the computation of the full scattering rate including all the scattering processes. We therefore review in the next sections the expression of the main scattering terms that appear in the right-hand side of Eq. (1).

III. SCATTERING IN THE CONDUCTION BAND

A. Electron-hole scattering

As we stressed in the introduction, plasma dynamics computations based on one single valence band and on the static screening approximation underestimate the efficiency of carrier-carrier scattering processes. To improve this model, we consider two valence bands and the dynamic screening. The heavy-hole band is parabolic, characterized by a single mass m_H. We use the following algebraic expression to reproduce approximately the nonlinearity of the light-hole dispersion curve:

$$\varepsilon_L(k) = \frac{\hbar^2}{2m_L}k^2 \frac{1}{1+\left[\frac{k}{k_c}\right]^2} + \left[\Delta E_{\text{HL}} + \frac{\hbar^2}{2m_H}k^2\right] \frac{\left[\frac{k}{k_c}\right]^2}{1+\left[\frac{k}{k_c}\right]^2} . \quad (13)$$

Around a critical vector $k_c \approx 3\times10^6/\text{cm}$ in GaAs, the light-hole band changes from a parabolic law (characterized by a small mass $m_L = 0.082$) to a curve of lower gradient which becomes quasiparallel to the heavy-hole band for $k > 5\times10^6/\text{cm}$ (see Fig. 3). The splitoff energy ΔE_{HL} between the two bands is of the order 70 meV. The anisotropy of the light-hole energy in K space is not taken into account by Eq. (13). We consider two classes of electron-hole collisions. In the first one, the hole stays in the same band (so-called in the following an "intravalence process"). In the second one, the hole is scattered from one valence band to the other one (so called in the following an "intervalence process"). Such processes are displayed in Fig. 3 for GaAs. The electron is scattered in the conduction band (process 1). Four hole processes may accompany this conduction transition (see labels

1a–1d in the valence bands), the initial state being either in the heavy- or in the light-hole band. The interband process (process 2) is characterized by the possibility of exchanging a larger energy and a smaller wave vector than for process 1. In this case, the hole scattering is only possible from the heavy-hole band to the light-hole band. Because of the small wave vector involved in process 2, such interband transitions are expected to be sensitive to dynamic effects of polarization (see the discussion in the previous section). We first compute the electron scattering rate due to interband processes such as 1a. The structure of the scattering rate is similar to that displayed in Eq. (3). $S_{i,j}^{-}$ and $S_{i,j}^{+}$ are, respectively, replaced by

$$S_{C,\mathrm{LH}}^{-}(k)=2\sum_{q}[1-f_c(E_C(\mathbf{k}-\mathbf{q}))]\sum_{k'}f_L(E_L(\mathbf{k}'))[1-f_H(E_H(\mathbf{k}'+\mathbf{q}))]$$
$$\times C_{\mathrm{LH}}(\mathbf{k}',\mathbf{k}'+\mathbf{q})\frac{2\pi}{\hbar}\left|\frac{V_0(q)}{\varepsilon(q,\Delta E)}\right|^2\delta[E_c(\mathbf{k})+E_L(\mathbf{k}')-E_c(\mathbf{k}-\mathbf{q})-E_H(\mathbf{k}'+\mathbf{q})] \tag{14}$$

and

$$S_{C,\mathrm{LH}}^{+}(k)=2\sum_{q}f_c(E_C(\mathbf{k}-\mathbf{q}))\sum_{k'}f_H(E_H(\mathbf{k}'+\mathbf{q}))[1-f_L(E_L(\mathbf{k}'))]$$
$$\times C_{\mathrm{LH}}(\mathbf{k}',\mathbf{k}'+\mathbf{q})\frac{2\pi}{\hbar}\left|\frac{V_0(q)}{\varepsilon(q,\Delta E)}\right|^2\delta[E_c(\mathbf{k})+E_L(\mathbf{k}')-E_c(\mathbf{k}-\mathbf{q})-E_H(\mathbf{k}'+\mathbf{q})]\ . \tag{15}$$

Some points are worthy of note. (1) There is no exchange term in the scattering amplitude. This is a crucial simplification with respect to intraband collisions as will be seen in Sec. III B. (2) $V_0(q)$ is the Fourier transform of the Coulomb potential, i.e., $V_0(q)=4\pi e^2/\varepsilon_0 q^2$. $C_{\mathrm{LH}}(\mathbf{k},\mathbf{k}+\mathbf{q})$ is the overlap coefficient already discussed [see Eq. (6)].

Following the calculation deferred to Appendix B, the expressions for the quantities $S_{C,\mathrm{LH}}^{\pm}(k)$ reduce to nasty triple integrals, namely,

$$S_{C,\mathrm{LH}}^{-}(\varepsilon)=K\int_0^{\infty}d\rho\int_{-1}^{+1}d\varphi[1-f_c(\varepsilon-\Delta E_c)]\frac{1}{\rho^2|\varepsilon(q,\Delta E_c)|^2}$$
$$\times d\lambda f_L\left[\varepsilon_L\left[\frac{1}{\hbar}(2m_H\lambda)^{1/2}\right]\right]\left[1-f_H\left[\varepsilon_L\left[\frac{1}{\hbar}(2m_H\lambda)^{1/2}\right]+\Delta E_c\right]\right]C_{\mathrm{LH}}(\rho,\lambda,\sigma)\ , \tag{16a}$$

$$S_{C,\mathrm{LH}}^{+}(\varepsilon)=K\int_0^{\infty}d\rho\int_{-1}^{+1}d\varphi f_c(\varepsilon-\Delta E_c)\frac{1}{\rho^2|\varepsilon(q,\Delta E_c)|^2}$$
$$\times\int_{D(\varepsilon,\rho,\sigma,\varphi)}d\lambda f_H\left[\varepsilon_L\left[\frac{1}{\hbar}(2m_H\lambda)^{1/2}\right]+\Delta E_c\right]\left[1-f_L\left[\varepsilon_L\left[\frac{1}{\hbar}(2m_H\lambda)^{1/2}\right]\right]\right]C_{\mathrm{LH}}(\rho,\lambda,\sigma)\ . \tag{16b}$$

We must also include the second scattering rate due to the interband process 1b as displayed in Fig. 3. Calculations are very similar to those of process 1a. Details are also reported in Appendix B.

Notice that the intravalence scattering factors $S_{C,\mathrm{HH}}^{\pm}(k)$ (i.e., when the hole stays in the heavy-hole band) can be easily derived from Eqs. (16) using the substitutions: subscript $L\rightarrow$subscript H; $\varepsilon_L\rightarrow\lambda$; $C_{\mathrm{LH}}\rightarrow C_{\mathrm{HH}}$. The integration interval $D(\varepsilon,\rho,\sigma,\varphi)$ over λ is determined by the simple condition $\lambda>(\sigma/\rho)[\varphi\sqrt{\varepsilon\rho}-\frac{1}{2}(1+1/\sigma)\rho]^2$.

B. Electron-electron scattering

The treatment of the electron-electron scattering (and the hole-hole scattering) is difficult because of the exchange interaction. The scattering rates $S_{C,C}^{\pm}$ are similar to those reported in Eqs. (14) and (15) and now read

$$S_{C,C}^{-}(k)=\sum_{q}[1-f_C(E_c(\mathbf{k}-\mathbf{q}))]\sum_{k'}f_C(E_c(\mathbf{k}'))[1-f_C(E_c(\mathbf{k}'+\mathbf{q}))]$$
$$\times\frac{2\pi}{\hbar}\left[\left|\frac{V_0(q)}{\varepsilon(q,\Delta E_{\mathrm{di}})}-\frac{V_0(\mathbf{k}-\mathbf{k}'-\mathbf{q})}{\varepsilon(\mathbf{k}-\mathbf{k}'-\mathbf{q},\Delta E_{\mathrm{ex}})}\right|^2+\left|\frac{V_0(q)}{\varepsilon(q,\Delta E_{\mathrm{di}})}\right|^2\right]\delta[E_c(\mathbf{k})+E_c(\mathbf{k}')-E_c(\mathbf{k}-\mathbf{q})-E_c(\mathbf{k}'+\mathbf{q})] \tag{17a}$$

and

$$S^{+}_{C,C}(k)=\sum_{q} f_C(E_c(\mathbf{k}-\mathbf{q}))\sum_{k'} f_C(E_c(\mathbf{k}'+\mathbf{q}))[1-f_c(E_c(\mathbf{k}'))] \times\frac{2\pi}{\hbar}\left[\left|\frac{V_0(q)}{\varepsilon(q,\Delta E_{\rm di})}-\frac{V_0(\mathbf{k}-\mathbf{k}'-\mathbf{q})}{\varepsilon(\mathbf{k}-\mathbf{k}'-\mathbf{q},\Delta E_{\rm ex})}\right|^2+\left|\frac{V_0(q)}{\varepsilon(q,\Delta E_{\rm di})}\right|^2\right]\delta[E_c(\mathbf{k})+E_c(\mathbf{k}')-E_c(\mathbf{k}-\mathbf{q})-E_c(\mathbf{k}'+\mathbf{q})] . \quad (17b)$$

Here $\Delta E_{\rm di}=E_C(\mathbf{k})-E_C(\mathbf{k}-\mathbf{q})$ and $\Delta E_{\rm ex}=E_C(\mathbf{k})-E_C(\mathbf{k}'+\mathbf{q})$ are the energies exchanged in the direct and exchange processes, respectively. The calculation of $S^{\pm}_{C,C}$ has been already carried out in the static approximation and reduces to triple integrals.[31] Now, the static screening approximation is in general not satisfactory for electrons in the Γ valley. To our knowledge, the full computation of the terms $S^{\pm}_{C,C}$ including both the exchange interaction and the dynamic screening has not been conducted. If the exchange contribution is omitted, the computation (including dynamic screening) is similar to that of the electron-hole collisions for parabolic bands (see Sec. III A). In this approximation, the scattering rate for electron-electron collisions can be derived from Eqs. (16) using the substitutions: subscript $L\rightarrow$ subscript C; subscript $H\rightarrow$ subscript C; $\sigma=1$, $\varepsilon_L=\lambda$, and $C_{\rm LH}\rightarrow C_{\rm CC}=1$. The integration interval $D(\varepsilon,\rho,\sigma,\varphi)$ over λ is defined by the simple relation $\lambda>[\varphi\sqrt{\varepsilon}-\sqrt{\rho}]^2$. The computation of the electron-electron scattering rate is, however, achieved with an accuracy that is not well characterized at high plasma density as will be seen below.

C. Emission of mixed LO-phonon plasmon modes

The scattering rate due to the emission-absorption of *bare* LO phonons has been already derived in Sec. II. Use Eqs. (4) and (5) with $C_{\rm CC}=1$. When the energy of the plasmon is not small compared to that of the LO phonon (typically at plasma densities larger that $10^{17}/{\rm cm}^3$ in GaAs), mixed LO-phonon plasmon modes are emitted by the carriers. The derivation of the corresponding scattering rate is deferred to Sec. IV B.

IV. SCATTERING IN THE VALENCE BAND

A. Intravalence hole-hole scattering

We restrict our analysis to the scattering of holes in the heavy-hole band. The computation of collision rates is similar to that of electrons in the conduction band except for the hole overlap coefficients $C_{\rm HH}$ which do not reduce to unity and must be explicitly taken into account [see Eq. (6)]. As a result, hole scattering calculations are more complex than those for electrons. The general computation of the hole-hole collision rate including both the exchange interaction and the dynamic approximation seems inextricable. Fortunately photogenerated holes are often cold and cannot exchange both an energy of the order of the plasmon and a wave vector smaller or of the order of the Debye-Hückel vector. The static screening therefore often holds for computing the hole-hole scattering rate. If the exchange term is omitted, because its inclusion even in the static screening is difficult, the scattering rate reads

$$S^{-}_{H,H}(k)=2\sum_{q}[1-f_H(E_H(\mathbf{k}-\mathbf{q}))]C_{\rm HH}(\mathbf{k},\mathbf{k}-\mathbf{q})\sum_{k'} f_H(E_H(\mathbf{k}'))[1-f_H(E_H(\mathbf{k}'+\mathbf{q}))]C_{\rm HH}(\mathbf{k}',\mathbf{k}'+\mathbf{q}) \times\frac{2\pi}{\hbar}\left|\frac{V_0(q)}{\varepsilon(q,\Delta E)}\right|^2\delta[E_H(\mathbf{k})+E_H(\mathbf{k}')-E_H(\mathbf{k}-\mathbf{q})-E_H(\mathbf{k}'+\mathbf{q})] . \quad (18)$$

The final expression of the scattering rate is very similar to that of the electron hole. Notice that the consideration of the two hole overlap coefficients $C_{\rm HH}$ in Eq. (18) typically reduces the scattering rate by a factor 10 with respect to the result obtained in the approximation $C_{\rm HH}=1$.

B. Emission of mixed LO-phonon plasmon modes

The scattering rate due to the emission absorption of *bare* LO phonons has already been derived in Sec. II. For holes, use Eqs. (4) and (5) with $C_{\rm HH}=C_{\rm LL}=(1+3\cos^2\chi)/4$ and $C_{\rm LH}=C_{\rm HL}=3\sin^2(\chi)/4$. When the energy of the plasmon is not small compared to that of the LO phonon (typically at plasma densities larger than $10^{17}/{\rm cm}^3$ in GaAs), mixed LO-phonon plasmon modes are emitted by the carriers or excitons [see for instance Refs. 46–48]. The emission rate is as previously determined by Eq. (3). In the following, the mixed mode energies and the mixed mode occupation functions are denoted ω_α and b_α, respectively. S^{+}_{ij} reads[48]

$$S^{+}_{ij}(k)=\frac{2\pi}{\hbar}\sum_{q,\upsilon=\pm,\alpha} f_j(\mathbf{k}-\mathbf{q})\left|\frac{V_{\rm LO}(q)}{\varepsilon_{\rm RPA}[q,\omega_\alpha(q)]}\right|^2 C_{ij}(\mathbf{k},\mathbf{k}-\mathbf{q})A_\alpha(q)\left[\frac{1}{2}-\upsilon\frac{1}{2}+b_\alpha(q)\right]\delta[\Delta E_{ij}(k)-\upsilon\hbar\omega_\alpha(q)] . \quad (19)$$

Equation (19) may be compared to Eqs. (4)–(7) that dealt with the emission of bare LO phonons. The energy of the mixed modes $\hbar\omega_\alpha(q)$ may be determined from the solution of the following equation:

$$\omega_\alpha^4(q)-[\omega_{\rm pl}^2(q)+\omega_{\rm LO}^2]\omega_\alpha^2(q)+\omega_{\rm LO}^2\omega_{\rm pl}^2(q)-\omega_{\rm LO}^2\omega_{\rm pl}^2(0)\left[1-\frac{\varepsilon_\infty}{\varepsilon_0}\right]=0 .$$

The coefficient $A_\alpha(q)$ in Eq. (19) is the renormalization factor of the Fröhlich interaction for the emission absorption of mixed modes. The expressions of $A_\alpha(q)$ in the plasmon pole approximation read

$$A_1(q)=\frac{\omega_{\rm LO}}{\omega_1(q)}\frac{\omega_1^2(q)-\omega_{\rm pl}^2(q)}{\omega_1^2(q)-\omega_2^2(q)} ,$$

$$A_2(q)=\frac{\omega_{\rm LO}}{\omega_2(q)}\frac{\omega_{\rm pl}^2(q)-\omega_2^2(q)}{\omega_1^2(q)-\omega_2^2(q)} .$$

V. RELAXATION OF CONDUCTION ELECTRONS IN INTRINSIC GaAs

As we stressed in Sec. III B, there exists so far no fully satisfactory computation of the *C-C* (and to some extent *H-H*) scattering rate because the exchange interaction and the dynamic screening have never been simultaneously taken into account. This problem is especially important for studying the dynamics of the photogenerated electrons in undoped GaAs when the *C-C* process becomes the dominant scattering process at plasma densities typically above $10^{-17}/\text{cm}^3$. We studied in Fig. 5 the efficiency of the *C-C* scattering rate by computing the relative scattering rate, i.e, the quantity $R_{\rm cc}=(1/f_c)/(df_c/dt)|_c$, just at the photogeneration energy E_p. This way, we get information about the rate of scattering of the conduction electrons *out* of their initial level. We chose a Lorentzian distribution of carriers with a broadening of 20 meV at half height that was centered around the photogeneration energy $E_p=60$ meV. The hole and electron densities were equal (intrinsic photoexcited material). Different models were compared. Square and triangular data points were computed using the dynamic and static screening, respectively. The exchange interaction was omitted in both cases. In the low-density limit (typically with $\rho<5\times10^{15}/\text{cm}^3$), these two calculations lead to similar results because the Debye-Hückel wave vector q_D is smaller than the wave vector exchanged in most of the collision processes (for instance, q_D equals 3.5×10^5/cm at $\rho=10^{16}/\text{cm}^3$). In other words, the choice of the screening model is not essential at low density. The diamond data points were computed to include the exchange term to the scattering amplitude in the framework of the static screening approximation. It turns out that, at low density (typically for $\rho<10^{16}/\text{cm}^3$), the scattering rate is very weakly enhanced (by 5–10 %) when the exchange is included. We therefore conclude that (i) including the exchange is not essential at low density to compute the *C-C* scattering rate; (ii) the static screening approximation may be used. In the high-density limit [for $\rho>(1-2)\times10^{16}/\text{cm}^3$], the dynamic enhancement of the Coulomb potential becomes important and the scattering rate in the framework of the dynamic screening without exchange (square data points in Fig. 5) exceeds the other ones (triangular and diamond data points). Notice that the full computation including, at high density, both the dynamic screening and the exchange is missing.

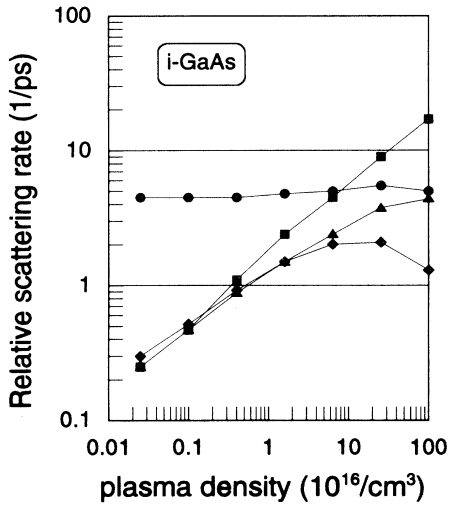

FIG. 5. Electron-electron scattering rate $R_{\rm cc}=(1/f_c)/(df_c/dt)|_c$ at the photogeneration energy vs the electron-hole plasma density. The electron distribution is centered around the photogeneration energy 60 meV with a broadening of 20 meV at half height. Square data points, dynamic screening approximation (PPA) without exchange; triangular points, static screening approximation without exchange; diamond data points, static screening with exchange. Circular data points, electron scattering rate $R_{C,\rm LO}=(1/f_c)/(df_c/dt)|_{\rm LO}$ by emission-absorption of bare LO phonons.

We also plotted the average scattering rate at the photogeneration energy due to the emission absorption of bare LO phonons [i.e., $R_{C,\rm LO}=(1/f_c)(df_c/dt)|_{\rm LO}$, circular data points in Fig. 5]. The scattering rate is quasiconstant for plasma densities ranging from 10^{15} to $10^{18}/\text{cm}^3$, except for a small enhancement around the density $(2-3)\times10^{17}/\text{cm}^3$ due to the phonon-plasmon resonance. The more sophisticated theory that considers the emission absorption of mixed LO-phonon plasmon modes provides very similar scattering rates for plasma densities lower that $10^{18}/\text{cm}^3$ in intrinsic GaAs (photogeneration energy 60–70 meV above the band edge).

We plotted in Fig. 6 the relative conduction-conduction scattering rate $R_{\rm cc}$ versus the initial photogeneration energy, for different plasma densities, namely, $\rho=2.5\times10^{16}/\text{cm}^3$, $\rho=10^{17}/\text{cm}^3$, and $\rho=4\times10^{17}/\text{cm}^3$. These curves provide an estimate of the internal thermalization time of the conduction electrons which is of the order of 1 or 2 times $1/R_{\rm cc}$. For instance, when the den-

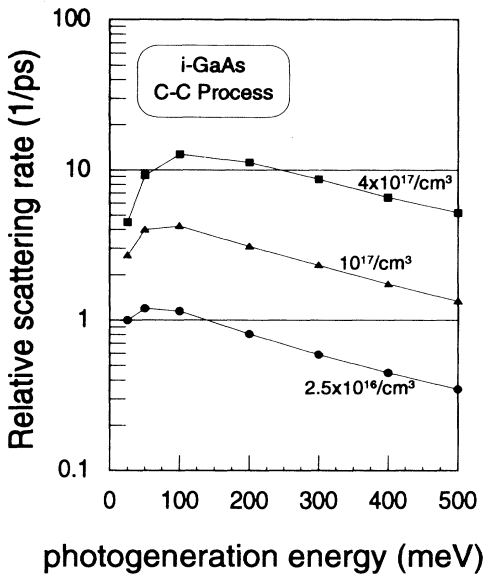

FIG. 6. Computation of the relative scattering rate $R_{cc}=(1/f_c)/(df_c/dt)|_c$ in the conduction band vs the initial photogeneration energy. The relative scattering rate is computed at the photogeneration energy using the dynamic screening. The broadening of the electron distribution at half height is 20 meV.

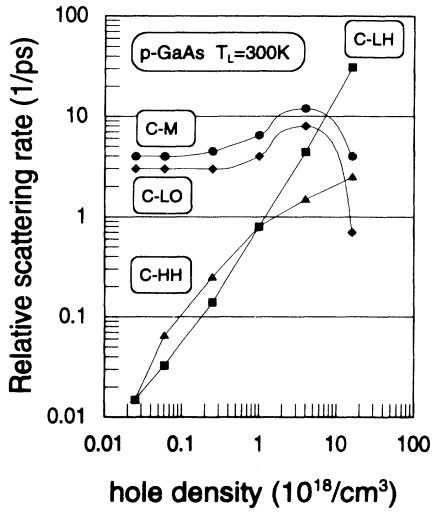

FIG. 7. Computation of the different relative scattering rates $R_{C,\mathrm{LH}}=(1/f_c)/(df_c/dt)|_{\mathrm{LH}}$, $R_{C,HH}=(1/f_c)/(df_c/dt)|_{\mathrm{HH}}$, $R_{C,\mathrm{LO}}=(1/f_c)/(df_c/dt)|_{\mathrm{LO}}$, and $R_{C,M}=(1/f_c)/(df_c/dt)|_M$ at the photogeneration energy vs the hole density in p-doped GaAs. All the processes are screened dynamically. Electrons are photogenerated with an initial energy of 400 meV. The broadening of the electron distribution is 50 meV. All scattering rates are computed using a dynamic screening.

sity is around $4\times10^{17}/\mathrm{cm}^3$ and the photogeneration energy around 50 meV, the internal thermalization time may be estimated to be of the order of 110–160 fs.

VI. RELAXATION OF CONDUCTION ELECTRONS IN p-DOPED GaAs

We showed in Sec. II that the e-h collisions accompanied by the excitation of a heavy hole into the light-hole band could be dynamically enhanced in *heavily* p-doped materials (say, for $\rho_h>4\times10^{18}/\mathrm{cm}^3$). We go now one step further by computing and comparing the different electron scattering rates just as the photogeneration energy. We recall that $R_{C\text{-HH}}$ and $R_{C\text{-LH}}$ are the relative scattering rates when the hole stays in the heavy-hole band [i.e., $R_{C,\mathrm{HH}}=(1/f_c)(df_c/dt)|_{\mathrm{HH}}$] or when the hole is scattered between the heavy- and light-hole bands, respectively. $R_{C\text{-LO}}$ and $R_{C,M}$ are the scattering rates due to the emission of LO phonons or mixed modes, respectively. The computed quantities $R_{C\text{-HH}}$, $R_{C\text{-LH}}$, $R_{C\text{-LO}}$, and $R_{C,M}$ enable us to determine on which time scale a scattering process may modify the conduction-band distribution at the photogeneration energy. We chose a Lorentzian conduction distribution with a broadening of 50 meV that is centered around the photogeneration energy $E_p=400$ meV (i.e., hot pumping). Holes are thermalized at the temperature of 300 K. The electron density is low, namely, $10^{14}/\mathrm{cm}^3$ so that the electron-electron collision rate is small compared to $R_{C\text{-LO}}$. Figures 7 and 8 display the relative scattering rates of the conduction electrons computed for dynamic and static screening, respectively. The following features should be noted.

(1) At low doping [below $(2-3)\times10^{16}/\mathrm{cm}^3$], the screening model is not essential as previously deduced for undoped GaAs. The reason is again that the Debye-Hückel wave vector q_D is smaller than the vector that is ex-

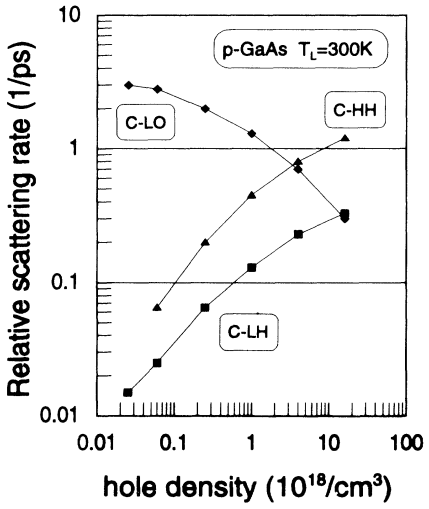

FIG. 8. Computation of the different relative scattering rates $R_{C,\mathrm{LH}}=(1/f_c)/(df_c/dt)|_{\mathrm{LH}}$, $R_{C,\mathrm{HH}}=(1/f_c)/(df_c/dt)|_{\mathrm{HH}}$, $R_{C,\mathrm{LO}}=(1/f_c)/(df_c/dt)|_{\mathrm{LO}}$, and $R_{C,M}=(1/f_c)/(df_c/dt)|_M$ at the photogeneration energy vs the hole density in p-doped GaAs. All the scattering processes are screened statistically. Electrons are photogenerated with an initial energy of 400 meV. The broadening of the electron distribution is 50 meV. All scattering rates are computed using a dynamic screening.

changed in most of the collision processes. The emission of LO phonons is by far the most efficient relaxation process for conduction electrons.

(2) At high density the behavior of the electron-hole processes are completely different in the static and dynamic screening approximations. Basically all the relative scattering rates increase sublinearly in a static screening model because of the increase of the Debye-Hückel wave vector reducing the matrix elements. The dynamic treatment of the C-HH process does not strongly increase the relative scattering rate of this process (compare the triangular data points in Figs. 7 and 8). For this type of collision between two particles of very different masses, the scattering cannot involve, simultaneously, the exchange of a wave vector smaller or of the order of the Debye-Hückel vector and the exchange of an energy close to that of the plasmon. On the contrary, these conditions are easily fulfilled by the C-LH process (see the discussion at the end of Sec. II) which is very sensitive to dynamic effects. The C-LH process increases sublinearly and becomes dominant above $10^{19}/\mathrm{cm}^3$ in dynamic screening (square data points in Fig. 7). $R_{C\text{-LH}}$ reaches 30/ps around $1.5\times10^{19}/\mathrm{cm}^3$ and increases further at higher densities.[49] This superlinear rise with increasing density is due to the dynamic enhancement because the energy $\Delta E\approx70$ meV that is exchanged when exciting a heavy hole into the light-hole band becomes close to that of the hole plasmon (see the discussion in Sec. II). Notice that to the contrary, the C-LH process always remains a minor process in static screening (Fig. 8). This result demonstrates the great impact of dynamic screening on the C-LH process.

(3) The density dependence of the scattering rate by emission absorption of *bare* LO phonons (C-LO process) is also completely different in static and dynamic screening models. For a dynamic screening, a peak is observed when the hole density is around $(5-6)\times10^{18}/\mathrm{cm}^3$, corresponding to the resonance of the LO-phonon energy with that of the hole plasmon (diamond data points in Fig. 7). The dynamic enhancement of the LO-phonon emission and the C-LO process is responsible for a net increase of the scattering of the conduction electrons in the Γ valley at density above $5\times10^{17}/\mathrm{cm}^3$ in p-doped GaAs.

(4) If we consider the scattering rate $R_{C,M}$ by emission-absorption of mixed LO-phonon plasmon modes (circular data points, Fig. 7), we get a slight increase of the scattering with respect to that of bare LO phonons but the results of the two theories are similar.

VII. CONCLUSION

This work was devoted to discussing plasma dynamics in relation to the screening and the exchange theories. Computations were dedicated to GaAs when the electron-hole plasma was generated with a limited initial kinetic energy and mostly stayed within the central Γ valley. We made a particular point of discussing the relative efficiency of the different scattering processes in the conduction band. The following conclusions hold.

(i) Relaxation of conduction electrons in intrinsic GaAs, photogeneration energy 60–70 meV above the band edge. (a) Conduction-conduction scattering. Dynamic screening is essential for calculating the C-C collision rate at densities above $(1-2)\times10^{16}/\mathrm{cm}^3$. For densities below $5\times10^{15}/\mathrm{cm}^3$, dynamic and static screening theories provide similar results. The consideration of the exchange term, that greatly complicates the calculations, gives rise to a small enhancement of the scattering rate at low density and therefore is not crucial. (b) Scattering by emission-absorption of bare LO phonons or mixed LO-phonon plasmon modes. The two theories lead to similar results. The relative scattering rate at the photogeneration energy is quasiconstant around 5 ps^{-1} for plasma densities ranging from 10^{15} to $10^{18}/\mathrm{cm}$.[3] The simple theory of *bare* LO-phonon emission without screening is reasonably good up to $(3-4)\times10^{17}/\mathrm{cm}^3$. (c) The static screening generally holds for H-H processes (heavy-hole–heavy-hole collisions).

(ii) Relaxation of conduction electrons in weakly excited p-doped GaAs (i.e., $\rho_c\ll\rho_h$). Holes remain thermalized at the bath temperature. The plasma dynamics following an excitation reduces to the thermalization and cooling of the electrons. The dynamic screening of the CC, C-LO processes is necessary. The relaxation of the photogenerated electrons by direct excitation of a heavy hole into the light-hole band becomes the dominant *intraband* relaxation process (C-HL process) for $\rho_h>(5-6)\times10^{18}/\mathrm{cm}^3$. In heavily p-doped material, the scattering rate $R_{C\text{-LH}}$ reaches 30/ps around the hole density $\rho_h\approx2\times10^{19}/\mathrm{cm}^3$ and therefore competes with the $\Gamma\rightarrow L$ or $\Gamma\rightarrow X$ intervalley transfers since $R_{\Gamma\rightarrow L}\approx10/\mathrm{ps}$ (Ref. 10) and $R_{\Gamma\rightarrow X}\approx30/\mathrm{ps}$.[6]

Further comparisons between experimental data and scattering rate computations are needed. We must stress, however, that an accurate experimental determination of the plasma density is *crucial* in order to compare theoretical kinetics to experimental data without adjusting the density.

ACKNOWLEDGMENTS

We are indebted to J. Kuhl, W. W. Rühle, X. Q. Zhou (Max Planck Institute, Stuttgart), and K. Leo (Institute for Semiconductor Electronics, Aachen) for many stimulating discussions and for communicating their experimental results prior to publication. We thank D. W. Snoke for stimulating discussions on carrier-carrier scattering at low density. We thank G. Bedford for a careful reading of the manuscript.

APPENDIX A

We recall that the application of the Boltzmann's equation is expected to hold for time $t>t_0$ where

$$t_0\approx1/q_D\bar{v}_{\mathrm{th}}\ . \tag{A1}$$

We estimate t_0 in the following.

Case 1: Nondegenerate regime close to thermalization. Here $1/q_D^2=\varepsilon_\infty K_BT/4\pi\rho e^2$ and $\bar{v}_{\mathrm{th}}=(8K_BT/\pi m)^{1/2}$. Condition (A1) becomes

$$t>t_0\approx\frac{1}{(q_D^2\bar{v}^2)^{1/2}}=\left[\frac{m\varepsilon_\infty}{12\rho e^2}\right]^{1/2}.$$

With typical parameters such as $\varepsilon=10$ and $m=0.086$ we get $t_0 \gg 50$ and 15 fs, respectively, for $\rho=10^{17}/\text{cm}^3$ and $\rho=10^{18}/\text{cm}^3$.

Case 2: Monokinetic distribution. We assume that all electrons have the same kinetic energy E_p. In that case, $1/q_D^2=\varepsilon_\infty E_p/2\pi\rho e^2$ and $\bar{v}_{\text{th}}=(2E_p/m)^{1/2}$. Condition (A1) becomes

$$t>t_0 \approx \frac{1}{(q_D^2\bar{v}^2)^{1/2}}=\left[\frac{m\varepsilon_\infty}{4\pi\rho e^2}\right]^{1/2} .$$

This condition is almost identical to that previously deduced in the quasithermalized regime.

APPENDIX B

1. Process 1a in Fig. 3

We derive in this appendix the Eqs. (16) for the electron-hole scattering rate. Let us compute first $S^-_{C,\text{LH}}(k)$. Using the expression for the Coulomb potential, Eq. (14) becomes

$$S^-_{C,\text{LH}}(k)=\frac{64\pi^3e^4}{\varepsilon_0^2\hbar V^2}\sum_q [1-f_c(E_C(\mathbf{k}-\mathbf{q}))]\frac{1}{q^4|\varepsilon(q,\Delta E_c)|^2}\sum_{k'} f_L(E_L(\mathbf{k}'))[1-f_H(E_H(\mathbf{k}'+\mathbf{q}))]$$
$$\times C_{\text{LH}}(\mathbf{k}',\mathbf{k}'+\mathbf{q})\delta[E_c(\mathbf{k})+E_L(\mathbf{k}')-E_c(\mathbf{k}-\mathbf{q})-E_H(\mathbf{k}'+\mathbf{q})] . \quad \text{(B1)}$$

We use the following condensed notations

$$\varepsilon=E_c(k) , \quad \rho=\frac{\hbar^2}{2m_c}q^2 , \quad \varphi=\cos\theta ,$$
$$\lambda=E_H(\mathbf{k}')=\frac{\hbar^2}{2m_H}k'^2 , \quad \sigma=\frac{m_H}{m_c} , \quad \varphi'=\cos\theta' . \quad \text{(B2)}$$

The energies ΔE_c and ΔE_h that are respectively exchanged by the electron and the hole read

$$\Delta E_c=E_c(k)-E_c(\mathbf{k}-\mathbf{q})=\frac{\hbar^2}{m_c}qk\cos\theta-\frac{\hbar^2}{2m_c}q^2=2\varphi\sqrt{\rho\varepsilon}-\rho , \quad \text{(B3a)}$$

$$-\Delta E_H=E_H(\mathbf{k}'+\mathbf{q})-E_L(k')=\frac{\hbar^2}{m_H}qk'\cos\theta'+\frac{\hbar^2}{2m_H}q^2+\frac{\hbar^2}{2m_H}k'^2-E_L(k')$$
$$=2\varphi'\left[\frac{\rho\lambda}{\sigma}\right]^{1/2}+\frac{\rho}{\sigma}+\lambda-\varepsilon_L\left[\frac{1}{\hbar}(2m_H\lambda)^{1/2}\right] . \quad \text{(B3b)}$$

As already stressed $C_{\text{LH}}(\mathbf{k}',\mathbf{k}'+\mathbf{q})$ equals $3\sin^2(\chi)/4$ [see Eq. (6)], where χ is the angle between $\mathbf{k}'$ and $\mathbf{k}'+\mathbf{q}$. C_{LH} can be easily expressed in terms of ρ, λ, σ, φ' because $\cos^2(\chi)$ may be written as

$$\cos^2(\chi)=\frac{[\mathbf{k}'\cdot(\mathbf{k}'+\mathbf{q})]^2}{k'^2(\mathbf{k}'+\mathbf{q})^2}=\frac{\sigma\lambda+2\varphi'\sqrt{\sigma\lambda\rho}+\varphi'^2\rho}{\sigma\lambda+2\varphi'\sqrt{\sigma\lambda\rho}+\rho}=\frac{(\sqrt{\lambda\sigma}+\varphi'\sqrt{\rho})^2}{(\sqrt{\lambda\sigma}+\varphi'\sqrt{\rho})^2+(1-\varphi'^2)\rho} . \quad \text{(B4)}$$

Using Eqs. (B2)–(B4), we get

$$S^-_{C,\text{LH}}(\varepsilon)=\frac{64\pi^3e^4}{\varepsilon_0^2\hbar V^2}\sum_q [1-f_c(\varepsilon-\Delta E_c)]\frac{\left[\frac{\hbar^2}{2m_c}\right]^2}{\rho^2|\varepsilon(q,\Delta E_c)|^2}\sum_{k'} f_L\left[\varepsilon_L\left[\frac{1}{\hbar}(2m_H\lambda)^{1/2}\right]\right]\left[1-f_H\left[\varepsilon_L\left[\frac{1}{\hbar}(2m_H\lambda)^{1/2}\right]+\Delta E_c\right]\right]$$
$$\times\frac{3}{4}(1-\cos^2\chi)\delta\left[2\varphi\sqrt{\rho\varepsilon}-\rho-2\varphi'\left[\frac{\rho\lambda}{\sigma}\right]^{1/2}-\frac{\rho}{\sigma}-\lambda+\varepsilon_L\left[\frac{1}{\hbar}(2m_H\lambda)^{1/2}\right]\right] .$$

Introducing continuous coordinates for the summation over $\mathbf{k}$ we get

$$S^{-}_{C,\mathrm{LH}}(\varepsilon)=\frac{16\pi e^4}{\varepsilon_0^2\hbar V}\left[\frac{\hbar^2}{2m_c}\right]^2\sum_q[1-f_c(\varepsilon-\Delta E_c)]\frac{1}{\rho^2|\varepsilon(q,\Delta E_c)|^2}\left[\frac{2m_H}{\hbar^2}\right]^{1.5}$$
$$\times\frac{1}{2}\int_0^\infty\sqrt{\lambda}\,d\lambda f_L\left[\varepsilon_L\left[\frac{1}{\hbar}(2m_H\lambda)^{1/2}\right]\right]\left[1-f_H\left[\varepsilon_L\left[\frac{1}{\hbar}(2m_H\lambda)^{1/2}\right]+\Delta E_c\right]\right]$$
$$\times\int_{-1}^{1}d\varphi'\frac{3}{4}(1-\cos^2\chi)\delta\left[2\varphi\sqrt{\rho\varepsilon}-\rho-2\varphi'\left[\frac{\rho\lambda}{\sigma}\right]^{1/2}-\frac{\rho}{\sigma}-\lambda+\varepsilon_L\left[\frac{1}{\hbar}(2m_H\lambda)^{1/2}\right]\right]. \tag{B5}$$

As already stressed, the condition of energy conservation

$$2\varphi\sqrt{\rho\varepsilon}-\rho-2\varphi'\left[\frac{\rho\lambda}{\sigma}\right]^{1/2}-\frac{\rho}{\sigma}-\lambda+\varepsilon_L\left[\frac{1}{\hbar}(2m_H\lambda)^{1/2}\right]=0$$

and the condition $-1<\varphi'<1$ reduce the integration interval $D(\varepsilon,\rho,\sigma,\varphi)$ over λ. The integration is restricted to the values of λ which satisfy the following inequality:

$$\varphi'=\frac{\sigma}{4\rho\lambda}\left[2\varphi\sqrt{\rho\varepsilon}-\rho-\frac{\rho}{\sigma}-\lambda+\varepsilon_L\left[\frac{1}{\hbar}(2m_H\lambda)^{1/2}\right]\right]^2\le 1\ . \tag{B6}$$

[The integration over φ' is straightforward and contributes for a factor $\frac{3}{8}\sqrt{\sigma/\rho\lambda}(1-\cos^2\chi)$ where $\cos^2\chi$ must be computed using (B4) with φ' given by Eq. (B6). Equation (B5) becomes

$$S^{-}_{C,\mathrm{LH}}(\varepsilon)=K\int_0^\infty d\rho\int_{-1}^{+1}d\varphi[1-f_c(\varepsilon-\Delta E_c)]\frac{1}{\rho^2|\varepsilon(q,\Delta E_c)|^2}$$
$$\times\int_{D(\varepsilon,\rho,\sigma,\varphi)}d\lambda f_L\left[\varepsilon_L\left[\frac{1}{\hbar}(2m_H\lambda)^{1/2}\right]\right]\left[1-f_H\left[\varepsilon_L\left[\frac{1}{\hbar}(2m_H\lambda)^{1/2}\right]+\Delta E_c\right]\right]C_{\mathrm{LH}}(\rho,\lambda,\sigma)\ , \tag{B7a}$$

$$S^{+}_{C,\mathrm{LH}}(\varepsilon)=K\int_0^\infty d\rho\int_{-1}^{+1}d\varphi f_c(\varepsilon-\Delta E_c)\frac{1}{\rho^2|\varepsilon(q,\Delta E_c)|^2}$$
$$\times\int_{D(\varepsilon,\rho,\sigma,\varphi)}d\lambda f_H\left[\varepsilon_L\left[\frac{1}{\hbar}(2m_H\lambda)^{1/2}\right]+\Delta E_c\right]\left[1-f_L\left[\varepsilon_L\left[\frac{1}{\hbar}(2m_H\lambda)^{1/2}\right]\right]\right]C_{\mathrm{LH}}(\rho,\lambda,\sigma)\ , \tag{B7b}$$

where $K=e^4m_h^2/\pi\varepsilon_0^2\hbar^3m_e\approx 13.1\times10^3(m_h^2/\varepsilon_0^2m_e)$ with m_h, m_e relative masses, ε_0: CGS, $S^{\pm}_{C,\mathrm{LH}}$ in units 1/ps. The dielectric function $\varepsilon(q,\Delta E)$ is computed using the plasmon pole approximation [see Eqs. (10)–(12)].

2. Process 1b (Fig. 3)

The algebraic treatment of this process is similar to that of process 1a. The expression for the energy that is exchanged in the conduction band is not modified [Eq. (B3a)]. In the valence band we get now [instead of Eq. (B3b)]

$$-\Delta E_H=E_L(k')-E_H(\mathbf{k}'-\mathbf{q})=E_L(k')-\frac{\hbar^2}{2m_H}k'^2+\frac{\hbar^2}{m_H}qk'\cos\theta'-\frac{\hbar^2}{2m_H}q^2$$
$$=\varepsilon_L\left[\frac{1}{\hbar}(2m_H\lambda)^{1/2}\right]-\lambda+2\varphi'\left[\frac{\rho\lambda}{\sigma}\right]^{1/2}-\frac{\rho}{\sigma}\ .$$

The energy conservation becomes

$$2\varphi\sqrt{\rho\varepsilon}-\rho-2\varphi'\left[\frac{\rho\lambda}{\sigma}\right]^{1/2}+\frac{\rho}{\sigma}-\varepsilon_L\left[\frac{1}{\hbar}(2m_H\lambda)^{1/2}\right]+\lambda=0\ .$$

The final result reads

$$S^{-}_{c\mathrm{HL}}(\varepsilon)=K\int_0^\infty d\rho\int_{-1}^{+1}d\varphi[1-f_c(\varepsilon-\Delta E_c)]\frac{1}{\rho^2|\varepsilon(\rho,\Delta E_c)|^2}$$
$$\times\int_{D(\varepsilon,\rho,\sigma,\varphi)}d\lambda f_H\left[\varepsilon_L\left[\frac{1}{\hbar}(2m_H\lambda)^{1/2}\right]-\Delta E_c\right]\left[1-f_L\left[\varepsilon_L\left[\frac{1}{\hbar}(2m_H\lambda)^{1/2}\right]\right]\right]C_{\alpha\beta}(\rho,\lambda,\sigma)\ ,$$

$$S_{c\mathrm{HL}}^{+}(\varepsilon)=K\int_0^{\infty}d\rho\int_{-1}^{+1}d\varphi\, f_c(\varepsilon-\Delta E_c)\frac{1}{\rho^2|\varepsilon(\rho,\Delta E_c)|^2}$$
$$\times\int_{D(\varepsilon,\rho,\sigma,\varphi)}d\lambda\, f_L\left[\varepsilon_L\left[\frac{1}{\hbar}(2m_H\lambda)^{1/2}\right]\right]\left[1-f_H\left[\varepsilon_L\left[\frac{1}{\hbar}(2m_H\lambda)^{1/2}\right]-\Delta E_c\right]\right]C_{\alpha\beta}(\rho,\lambda,\sigma)\ .$$

$D(\varepsilon,\rho,\sigma,\varphi)$ is here restricted to the values of λ which satisfy the following inequality:

$$\frac{\sigma}{4\rho\lambda}\left[2\varphi\sqrt{\rho\varepsilon}-\rho+\frac{\rho}{\sigma}+\lambda-\varepsilon_L\left[\frac{1}{\hbar}(2m_H\lambda)^{1/2}\right]\right]^2\le 1\ .$$

[1]C. V. Shank, R. L. Fork, R. F. Leheny, and J. Shah, Phys. Rev. Lett. **42**, 112 (1979).

[2]R. F. Leheny, J. Shah, R. L. Fork, C. V. Shank, and A. Migus, Solid State Commun. **31**, 809 (1979).

[3]J. L. Oudar, D. Hulin, A. Antonetti, and F. Alexandre, Phys. Rev. Lett. **55**, 2074 (1985).

[4]W. Z. Lin, J. G. Fujimoto, and E. P. Ippen, Appl. Phys. Lett. **50**, 124 (1986).

[5]R. W. Schoenlein, W. Z. Lin, E. P. Ippen, and J. G. Fujimoto, Appl. Phys. Lett. **51**, 1442 (1987).

[6]P. C. Becker, H. L. Fragnito, C. H. Brito Cruz, J. Shah, R. L. Fork, J. E. Cunningham, J. E. Henry, and C. V. Shank, Appl. Phys. Lett. **53**, 2089 (1988).

[7]X. Q. Zhou, G. C. Cho, U. Lemmer, W. Kütt, K. Wolter, and H. Kurz, Solid State Electron. **32**, 1591 (1989).

[8]C. W. W. Bradley, R. A. Taylor, and J. F. Ryan, Solid State Electron. **32**, 1173 (1989).

[9]H. Roskos, B. Rieck, A. Seilmeier, W. Kaiser, and G. G. Baumann, Phys. Rev. B **40**, 1396 (1989).

[10]J. Nunnemkamp, J. H. Collet, J. Klebniczki, J. Kuhl, and K. Ploog, Phys. Rev. B **43**, 14 047 (1991).

[11]J. C. Tsang and J. A. Kash, Phys. Rev. B **34**, 6003 (1986).

[12]J. A. Kash, Phys. Rev. B **40**, 3455 (1989).

[13]D. Bloch, J. Shah, and A. C. Gossard, Solid State Commun. **59**, 537 (1986).

[14]D. Y. Oberli, J. Shah, and T. C. Damen, Phys. Rev. B **40**, 1323 (1989).

[15]J. Shah, J. B. Devaud, T. C. Dammen, W. Tang, A. C. Gossard, and P. Lugli, Phys. Rev. Lett. **59**, 222 (1987).

[16]D. W. Snoke, W. W. Rühle, Y. C. Lu, and E. Bauser, Phys. Rev. B **45**, 10 979 (1992).

[17]P. C. Becker, H. L. Fragnito, C. H. Brito Cruz, J. Shah, R. L. Fork, J. E. Cunningham, J. E. Henry, and C. V. Shank, Appl. Phys. Lett. **53**, 2089, (1989).

[18]X. Q. Zhou, U. Lemmer, K. Seibert, G. C. Cho, W. Kütt, K. Wolter, and H. Kurz, in *Proceedings of the 20th International Conference on Semiconductors,* edited by E. M. Anastassakis and J. D. Joannopoulos (World Scientific, Singapore, 1990), p. 2522.

[19]R. Zimmermann, *Many Particle Theory of Excited Semiconductors* (Treubner Texte zur Physik, Leipzig, 1988).

[20]H. Haug, and S. Koch, *Quantum Theory of the Optical and Electronic Properties of Semiconductors* (World Scientific, Singapore, 1990).

[21]L. Boltzmann, Wiener Ber. **66**, 275 (1872) [English translation in *Kinetic Theory II,* edited by S. G. Brush (Pergamon, Oxford, 1966)].

[22]O. Penrose, Rep. Prog. Phys. **42**, 1937 (1979).

[23]L. P. Kadanoff and G. Baym, *Quantum Statistical Mechanics* (Benjamin, New York, 1963); J. Math. Phys. **3**, 605 (1968).

[24]L. V. Keldysh, Zh. Eksp. Teor. Fiz. **47**, 1515 (1964) [Sov. Phys. JETP **20**, 1018 (1965)].

[25]L. Landau and E. M. Lifshitz, *Course of Theoretical Physics* (Pergamon, Oxford, 1981), Vol. 10, Chap. X.

[26]R. Balescu, *Statistical Physics of Charged Particles* (Interscience, London, 1963).

[27]A. G. Hall, Mol. Phys. **28**, 1 (1974).

[28]K. Henneberger and V. Maj, Physica A **138**, 537 (1986).

[29]H. Glaeske and M. Schubert, Phys. Status Solidi B **145**, 385 (1988).

[30]K. Henneberger and H. Haug, Phys. Rev. B **38**, 9759 (1988).

[31]J. H. Collet and T. Amand, Physica B **134**, 394 (1985).

[32]J. H. Collet and T. Amand, J. Phys. Chem. Solids **47**, 153 (1986).

[33]J. H. Collet, J. L. Oudar, and T. Amand, Phys. Rev. B **34**, 5443 (1986).

[34]P. Lugli, Appl. Phys. Lett. **50**, 1521 (1987).

[35]R. P. Joshi, R. O. Grondin, and D. K. Ferry, Phys. Rev. B **42**, 692 (1990).

[36]A. D. W. Bailey, C. J. Stanton, and K. Hess, Phys. Rev. B **42**, 3423 (1990).

[37]M. Mosko and A. Moskova, Phys. Rev. B **44**, 10 794 (1991).

[38]U. Hohenester, P. Supancic, P. Kocevar, X. Q. Zhou, U. Lemmer, W. Kütt, and H. Kurz, Semicond. Sci. Technol. **7**, B176 (1992).

[39]A. Akhiezer and S. Peleminski, *Methods of Statistical Physics,* International Series in Natural Philosophy Vol. 104 (Pergamon, New York, 1981).

[40]J. D. Wiley, Phys. Rev. B **4**, 2485 (1971).

[41]C. Ehrenreich and M. H. Cohen, Phys. Rev. **115** 786 (1959).

[42]G. Mahan, *Many Particle Physics* (Plenum, New York, 1983).

[43]D. Yevick and W. Bardyszewski, Phys. Rev. B **39**, 8605 (1989).

[44]T. M. Rice, Nuovo Cimento B **23**, 226 (1974).

[45]Tran Thoai and H. Haug, Phys. Status Solidi (B) **98**, 581 (1980).

[46]H. Saito, Solid State Commun. **39**, 71 (1981).

[47]A. A. Klochikin, B. S. Razbirin, T. Amand, J. H. Collet, M. Pugnet, A. Cornet, and M. Brousseau, J. Phys. C **19**, 4237 (1986).

[48]S. Das Sharma, J. K. Jai, and R. Jalabert, Phys. Rev. B **41**, 3461 (1990).

[49]The consideration of the overlap factor C_{LH} in the scattering rates has typically reduced the scattering rate by a factor 8–10 with respect to a crude computation carried out with $C_{\mathrm{HL}}=1$.